

## Atomistic nature of NaCl nucleation at the solid-liquid interface

Yong Yang

*Institute of Physics, Chinese Academy of Sciences, Box 603, Beijing 100080, China*

Sheng Meng

*Physics Department, Harvard University, Cambridge, Massachusetts 02138*

(Received 22 August 2006; accepted 7 December 2006; published online 29 January 2007)

The early stage of heterogeneous nucleation of NaCl from supersaturated NaCl aqueous solution at the water-NaCl (001) interface has been investigated by molecular dynamics simulations. The critical size of the nuclei for spontaneous growth was found to be as small as two atoms (a  $\text{Na}^+$ - $\text{Cl}^-$  ion pair) at high supersaturation. Due to the presence of a relatively stable water network and the effect of the hydration force at the interface, the stable nuclei formed on the NaCl (001) are found to contain more  $\text{Na}^+$  ions than  $\text{Cl}^-$  ions. The different deposition characteristics of the  $\text{Na}^+$  and  $\text{Cl}^-$  solutes lead to a positively charged substrate and thus may introduce another driving force for nucleation besides the level of solution supersaturation. The role of water was further confirmed by comparison with NaCl epitaxy growth in the vacuum. © 2007 American Institute of Physics. [DOI: 10.1063/1.2431363]

### I. INTRODUCTION

The nucleation phenomena of crystals are of great importance in science and technology. During the past decades, extensive theoretical and experimental investigations were carried out to study the nucleation process and dynamics.<sup>1-10</sup> Despite the well-established models based on thermodynamics and kinetic rate equations,<sup>11</sup> little is known about these processes at the atomic level.<sup>12</sup> Due to the great challenge in the experimental measurement of atomic processes in solutions, computer simulations based on atomistic models have become efficient and powerful approaches. For example, the spontaneous nucleation of sodium chloride in a supersaturated aqueous solution has been investigated using molecular dynamics (MD) simulations by Ohtaki and Fukushima<sup>9</sup> and recently by Zahn.<sup>10</sup> Microclusters with irregular shapes were observed at the very early stage of nucleation. Most centers of the stable aggregates were found to be a nonhydrated  $\text{Na}^+$  ion that is octahedrally coordinated by six  $\text{Cl}^-$  ions.<sup>9,10</sup> In real-world applications of crystal growth, a seed crystal is usually used in the supersaturated solution, and the solutes nucleate gradually onto its surface and grow up. Different from the homogeneous nucleation as discussed in Refs. 9 and 10, the heterogeneous nucleation has a lower energy barrier and smaller critical size.<sup>8</sup> Upon this approach, crystals of better quality can be obtained than those from the homogeneous nucleation in solutions. However, this phenomenon, i.e., the nucleation process at the water-crystal interface, which is practically more relevant and important, remains unexplored at the molecular level. Oyen and Hentschke had studied the NaCl (001) surface in contact with aqueous NaCl solutions of various concentrations, but did not observe any crystallization at the interface.<sup>13</sup> The aim of this work is to investigate the early stage of nucleation of NaCl at the water-NaCl (001) interface.

### II. METHODS AND MODELS

The MD simulations were carried out using the AMBER 6.0 program.<sup>14</sup> The validity of the model potentials in AMBER 6.0 has been tested by *ab initio* calculations for ion-water clusters and the adsorption geometries of water molecules on the NaCl (001) surface. Good agreements are obtained.<sup>15</sup> The seed crystal used in our simulations is modeled by a five-layer NaCl (001) slab that consists of 160 NaCl units. Both sides of the slab are in contact with NaCl solution. At room temperature ( $\sim 298$  K), the concentration of saturated NaCl aqueous solution is 35.96 g/(100 ml  $\text{H}_2\text{O}$ ),<sup>16</sup> and the ratio between the number of NaCl units and water molecules is about 1/9. The supersaturated solution here contains 100 NaCl units and 600 water molecules. Using the mole fraction definition,<sup>16</sup> the supersaturation [ $\sigma = (c - c_0)/c_0$ , where  $c_0$  is the concentration of saturated solution, and  $c$  is the real concentration<sup>17</sup>] of the solution is calculated to be  $\sim 43\%$  ( $\sigma = [100/(100 + 600) - 1/(1 + 9)]/[1/(1 + 9)] \approx 0.43$ ). The water-water interaction is described by the TIP3P model,<sup>18</sup> and ion-ion and ion-water interactions are given by the PARM94 force field in AMBER 6.0 (Ref. 14) (details about the size and energy parameters of ions can be found in Ref. 19). The TIP3P water model<sup>18</sup> is used here because the ionic solution properties show little dependence on polarizability<sup>20</sup> while the polarization calculation is expensive in AMBER 6.0.<sup>14</sup> Eight systems, which have the same number of water and ions but different initial ionic positions and velocities, were used as the starting configurations for the simulations. All these systems were prepared in a supercell with most of the solutes coordinated by water molecules and then equilibrated at  $\sim 300$  K for at least 300 ps with harmonic restraints applied on the  $\text{Na}^+$  and  $\text{Cl}^-$  solutes during the equilibration procedure, before the production run started. The water molecules and the substrate were allowed to fully relax during the equilibration procedure. During the *N-P-T* (canonical ensemble with constant pressure) simulations, the size of the

unitcell fluctuates around  $22.83 \times 22.83 \times 62.76 \text{ \AA}^3$  with an amplitude less than  $0.5 \text{ \AA}$ . The Ewald summation<sup>21,22</sup> was applied to energy and force calculations with a cutoff of  $9 \text{ \AA}$  in real space. A time step of  $0.5 \text{ fs}$  was used, and the OH vibrations were frozen using the SHAKE algorithm.<sup>23</sup> The trajectories were recorded every  $30 \text{ fs}$  at  $\sim 300 \text{ K}$ . The temperature and pressure were controlled by the Berendsen's thermostat and barostat,<sup>24</sup> respectively, toward the target value of  $300 \text{ K}$  and  $1 \text{ bar}$ .

### III. RESULTS AND DISCUSSION

#### A. Critical nucleus size

According to classical nucleation theory,<sup>25</sup> small crystal nuclei form spontaneously in supersaturated solutions. The size of the nuclei must exceed a critical value, the so-called critical nucleus, beyond which the nuclei would continue to grow rather than decay into the solution.<sup>6,26</sup> We first studied the critical size of NaCl nucleation at the NaCl-water interface from molecular dynamics simulations. All the trajectories with different initial configurations and velocities were simulated for  $1.2 \text{ ns}$ . The nuclei size consisting of one, two, and three atoms, were counted during the MD simulation to obtain statistics. The statistics were made for the sum of the created and decayed nuclei, as shown in Fig. 1 and Table I. In the statistical analysis, a  $\text{Na}^+$  ( $\text{Cl}^-$ ) ion was considered as adsorbed on the NaCl (001) surface when the distance between the ion and the surface is less than  $3.25 \text{ \AA}$  (the first minimum of the radial distribution function  $g_{\text{Na-Cl}}$ ), while they were considered to leave the NaCl (001) surface when the distance is larger than  $5.5 \text{ \AA}$ , at which a  $\text{Na}^+-\text{Cl}^-$  bond is broken.<sup>20</sup> The same criterion was applied for the ionic bonds formed between the adsorbed solutes on the NaCl (001) surface in determining the size of the nuclei. In the following discussion, we will use the total numbers of the created and decayed nuclei within  $1.2 \text{ ns}$  simulations to determine the critical size. A nucleus is considered to be decayed when one or more atom(s) is (are) detached from it during this period. In Fig. 1, each data point represents a sum of created (decayed) nuclei from the beginning of the simulations. For the single-atom nuclei [one  $\text{Na}^+$  or one  $\text{Cl}^-$ , Fig. 1(a) and Table I], the sum of the created  $\text{Na}^+$  ( $\text{Cl}^-$ ) nuclei is 138 (110) during the  $1.2 \text{ ps}$  simulations, and the sum of the decayed  $\text{Na}^+$  ( $\text{Cl}^-$ ) nuclei is 74 (77). The probability of decay:  $P_{\text{decayNa1}} = 74/138 = 0.54 > 0.5$  and  $P_{\text{decayCl1}} = 77/110 = 0.7 > 0.5$ . For the two-atom nuclei [a  $\text{Na}^+-\text{Cl}^-$  pair in Fig. 1(b)], the probability of decay:  $P_{\text{decay2}} = 40/90 = 0.44 < 0.5$ . This is the critical size. For the three-atom nuclei [two  $\text{Na}^+$  with one  $\text{Cl}^-$  or two  $\text{Cl}^-$  with one  $\text{Na}^+$ , Fig. 1(c)] the probability of decay:  $P_{\text{decay3}} = 23/69 = 0.33 < P_{\text{decay2}} < 0.5$ . This tendency is consistent with the classical nucleation theory.<sup>25</sup> Once a nucleus has a larger size that exceeds the critical size, it has higher probability to grow at the water-NaCl interface. The critical size obtained here should be dependent on simulation details such as the level of supersaturation and the temperature. For example, in mid-level supersaturation solution (85 NaCl solutes, 600  $\text{H}_2\text{O}$ , and 24% supersaturation), the critical size at  $300 \text{ K}$  is found to be three atoms (one  $\text{Na}^+$  with

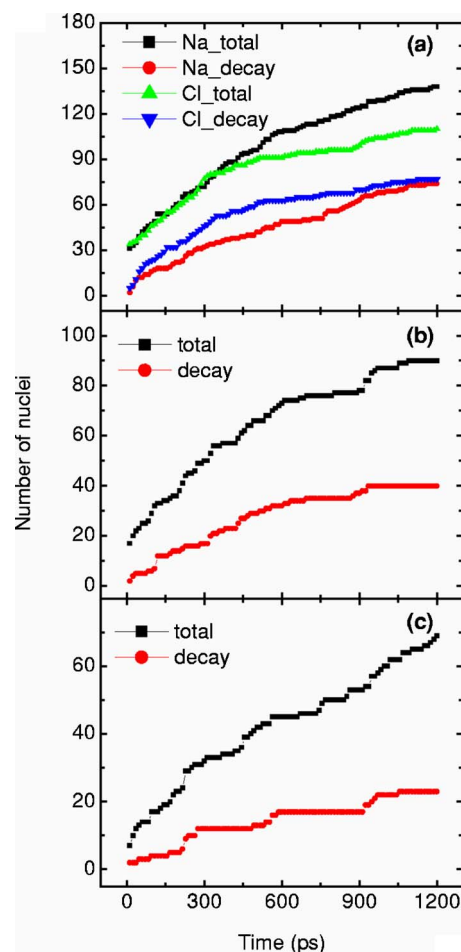


FIG. 1. (Color online) Time evolution of the total created and decayed nuclei during the MD simulations: (a) one-atom nuclei, (b) two-atom nuclei, and (c) three-atom nuclei. The statistics were done for eight different trajectories up to  $1.2 \text{ ns}$ .

two  $\text{Cl}^-$  or one  $\text{Cl}^-$  with two  $\text{Na}^+$ ). This is reasonable because the critical size will increase when the level of supersaturation is decreased (see Appendix).

Figure 2 shows a few snapshots of the growth for a typical two-atom nucleus at the water-NaCl (001) interface. It evolves from the two-atom nucleus [Fig. 2(a)] to a zigzag chain [(b)], and then to a three-dimensional (3D) island with increasing size [(c) and (d)]. For illustration, the two atoms in the nucleus are labeled as “1” ( $\text{Na}^+$ ) and “2” ( $\text{Cl}^-$ ). The statistics on the stable islands, whose size are larger than the critical size, shows that the number of Cl-centered nuclei is larger than the Na-centered nuclei. The number of  $\text{Cl}^-$  ions adsorbed on the NaCl (001) is less than  $\text{Na}^+$  ions, as can be seen from Figs. 2(c) and 2(d). In simulations longer than  $3 \text{ ns}$ , we have observed larger islands than the one shown in

TABLE I. Statistics on the sum of created and decayed one-atom, two-atom, and three-atom nuclei during the  $1.2 \text{ ns}$  MD simulations. The summation was done for eight different MD trajectories.

	One-atom $\text{Na}^+$	One-atom $\text{Cl}^-$	Two atom	Three atom
$N_{\text{total}}$	138	110	90	69
$N_{\text{decay}}$	74	77	40	23
$P_{\text{decay}}$	0.54	0.7	0.44	0.33

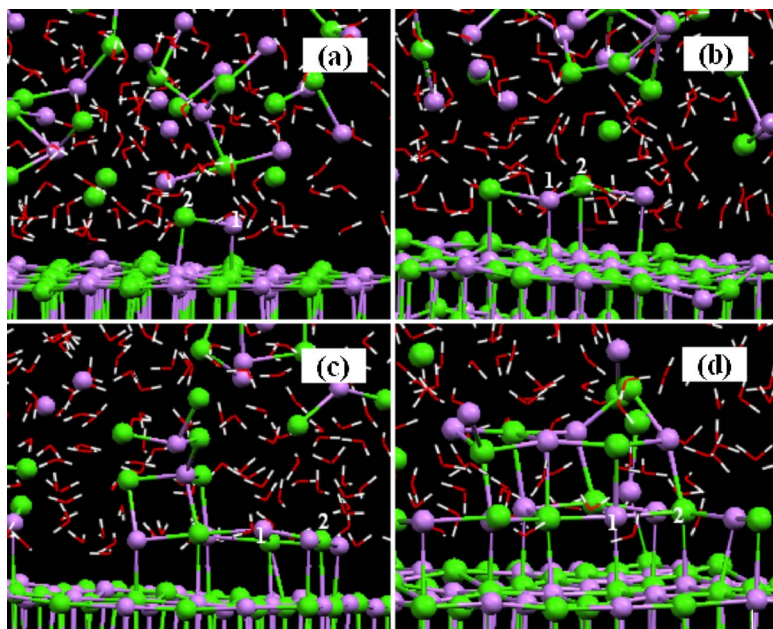


FIG. 2. (Color online) The growth of a two-atom nucleus ( $\text{Na}^+$  is labeled by “1” and  $\text{Cl}^-$  is labeled by “2”) evolved as a function of time. The  $\text{Na}^+$  and  $\text{Cl}^-$  ions are represented by purple (smaller) and green (larger) balls. Water molecules are represented by sticks, white for hydrogen, and red for oxygen. The snapshots were taken at (a)  $t=0.3$  ps (300 K), (b) 19.59 ps (300 K), (c) 1200 ps (300 K), and (d) 2550 ps (320 K).

Fig. 2(d). The maximum coordination ions for the  $\text{Na}^+$  and  $\text{Cl}^-$  in the islands are both six, the same as the bulk case.

## B. Coulombic driving forces for initial nucleation

Figure 3(a) gives the evolution of the average number of the deposited  $\text{Na}^+$  and  $\text{Cl}^-$  ions at the water- $\text{NaCl}$  (001) interface. The  $\text{Na}^+$  ions show a higher deposition rate than the  $\text{Cl}^-$  ions, leading to a larger number of  $\text{Na}^+$  ions. There is a small dip at  $t \sim 925$  ps in the  $\text{Na}^+$  deposition rate, after which

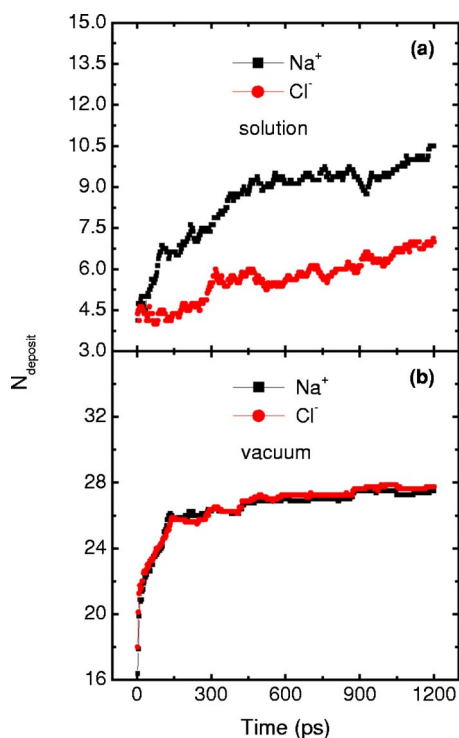


FIG. 3. (Color online) The total numbers of the deposited  $\text{Na}^+$  and  $\text{Cl}^-$  ions from aqueous solution (a) and vacuum (b) onto the  $\text{NaCl}$  (001) surface as a function of time. Each point represents the average of eight different simulation trajectories.

the number of deposited  $\text{Cl}^-$  ions increases rapidly again, followed by the further increase of deposited  $\text{Na}^+$  numbers. It seems to induce another cycle of  $\text{Na-Cl}$  deposition. The total number of deposited  $\text{Na}^+$  ions is always much larger than  $\text{Cl}^-$  ions during the 1.2 ns simulation. Moreover, this tendency shows no dependence on the ratio of  $\text{Na}^+$  and  $\text{Cl}^-$  solutes that might adsorb on the substrate during the equilibration process. It suggests that the water- $\text{NaCl}$  (001) interface is positively charged in the early stage of nucleation. The accumulation of positive charge at the interface will attract the  $\text{Cl}^-$  ions to deposit onto the seed crystal. This is observed for the first time and we suggest that it may serve as another driving force for nucleation from the solution in addition to the chemical potential difference in the classical nucleation theory.<sup>25</sup> For comparison, the MD simulations of the  $\text{NaCl}$  epitaxy (the same substrate and solutes) in the vacuum at  $\sim 300$  K is shown in Fig. 3(b). The depositions of  $\text{Na}^+$  and  $\text{Cl}^-$  are almost the same, which leads to a charge-neutral substrate. This implies that the  $\text{Na}^+$  and  $\text{Cl}^-$  ions are more likely to deposit onto the substrate in the form of neutral ion pairs, which are energetically favored in the vacuum than single ions. This shows clearly the role of water in the early stage of crystal growth at the solid-liquid interface.

From Figs. 1 and 3, the nucleation and deposition rates are larger in the first 300 ps than other simulation time. This is due to the fast decrease of supersaturation. The nucleation rate in the supersaturated solution is proportional to supersaturation.<sup>17</sup> At  $t \sim 300$  ps, the average deposition number of  $\text{Na}^+$  is  $\sim 7.5$ , and is  $\sim 6$  for  $\text{Cl}^-$ , and the level of supersaturation dropped from 43% to  $\sim 30\%$ , correspondingly.

## C. Relatively stable interfacial water networks

The different deposition characteristics of  $\text{Na}^+$  and  $\text{Cl}^-$  ions originate from the fact that a relatively stable water network presents at the liquid-solid interface, as shown in Fig. 4. When the solute  $\text{Na}^+$  ions approach the  $\text{NaCl}$  (001),



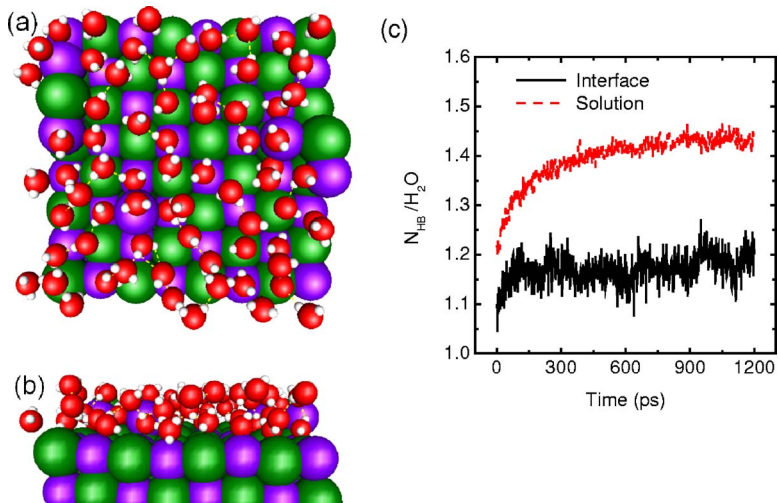


FIG. 4. (Color online) (a) Top and (b) side views of the water network near the NaCl (001) surface. The snapshot was taken at  $t=577.5$  ps for one side of the NaCl (001). The hydrogen bonds formed between the water molecules are indicated by dotted lines. (c) Time evolution of the average number of hydrogen bond per water at the interface and inside solution. The increasing trend of  $N_{HB}$  in solution is due to the continuous nucleation at the interface and inside solution. The decrease/increase of  $N_{HB}$  for interface water corresponds to ion deposition/dissolution during the 3D growth mode of NaCl nuclei on NaCl (001).

most of them will replace the water molecules atop the Cl<sup>-</sup> at the water-NaCl (001) interface because of the Coulombic interaction between Na<sup>+</sup> and Cl<sup>-</sup> ions. For the same reason, most of the solute Cl<sup>-</sup> ions prefer to replace the water molecules adsorbed atop the Na<sup>+</sup>. However, the water molecules on Cl<sup>-</sup> are stabilized via the H–Cl<sup>-</sup> hydrogen bonding, while they are bound through the O–Na<sup>+</sup> interactions on top of Na<sup>+</sup>, which are much stronger than the H–Cl<sup>-</sup> hydrogen bond. By *ab initio* calculation for a water monomer on NaCl (001), we found the adsorption energy differs by  $\sim 2.3$  times for water on Cl<sup>-</sup> (0.174 eV) and on Na<sup>+</sup> (0.401 eV).<sup>15</sup> From Fig. 4 one can see that most water molecules reside atop Na<sup>+</sup> rather than Cl<sup>-</sup>. The averaged resident time of the water molecules on the top sites of the surface Na<sup>+</sup> is calculated to be 8.95 ps, while the averaged resident time of the ones atop the surface Cl<sup>-</sup> is about 4.12 ps. These results demonstrate that the water molecules adsorbed on the top sites of the surface Na<sup>+</sup> are more stable than the ones adsorbed atop the surface Cl<sup>-</sup>. Another factor is the deposition flux of the solute Na<sup>+</sup> and Cl<sup>-</sup> ions, which is proportional to the averaged velocities of ions' thermal motions. The solute Na<sup>+</sup> has the same averaged kinetic energies as Cl<sup>-</sup> but larger averaged velocities and higher deposition flux because of its smaller mass. This is different from vacuum epitaxy because most Na<sup>+</sup> and Cl<sup>-</sup> ions are separated by water molecules. As a result, the Na<sup>+</sup> ions in the supersaturated solution have better chance to approach and stay on the NaCl (001) surface and show larger deposition rate (Fig. 3) at the interface than the Cl<sup>-</sup> ions. Further analysis shows that the water network is confined within a distance of no more than 5.5 Å to the water-NaCl (001) interface, which is a quasibilayer structure in the normal direction of the NaCl (001) surface [Figs. 4(a) and 4(b)]. In the solution the diffusion coefficient of single water molecule is calculated to be  $4.77 \times 10^{-9} \text{ m}^2 \text{ s}^{-1}$  [the value for TIP3P model in pure liquid water is  $\sim 5.5 \times 10^{-9} \text{ m}^2 \text{ s}^{-1}$  Ref. 27], while it is  $3.02 \times 10^{-9} \text{ m}^2 \text{ s}^{-1}$  when the water molecule presents in the interface water network. The detailed analysis in Fig. 4(c) shows that the average hydrogen bonds (HB) between water molecules is  $\sim 1.4 \text{ HB}/\text{H}_2\text{O}$  in solution, while it is only  $\sim 1.2 \text{ HB}/\text{H}_2\text{O}$  in the interfacial water network, due to the strong surface-water bonds that deteriorate the interface hydrogen bond network. For comparison, in an ideal ice

structure the number of HB is 2 in bulk and 1.75 at surface. Furthermore, an experimental evidence of such ordered water network at the water-NaCl (001) interface was found by surface x-ray diffraction.<sup>28</sup>

Because the solubility of the NaCl crystals shows minor dependence on temperature, one expects a very small change in the level of supersaturation when the solution temperature is increased to an appropriate higher value. For example, the solubility of NaCl is 35.65 g/100 ml H<sub>2</sub>O at  $\sim 273$  K, and is 38.99 g/100 ml H<sub>2</sub>O at  $\sim 373$  K,<sup>16</sup> corresponding to a molar ratio of  $N(\text{NaCl}):N(\text{H}_2\text{O})=1:9.1$  and  $1:8.3$ , respectively. However, the solutes and the water molecules exhibit higher mobility as temperature increases. The influence of the water network is thus reduced and the deposition rate of the solutes is increased. To demonstrate this, we gradually increased the solution temperature from 300 to 320 K in simulations after 1.2 ns. The rates of Na<sup>+</sup> and Cl<sup>-</sup> depositions are found to be larger than that at 300 K. Moreover, at the interface there exhibits a 3D growth mode, as schematically shown in Fig. 2(d). Keeping the NaCl substrate and solutes, the 3D growth mode is also observed in our MD simulations of the homogeneous epitaxy of NaCl in vacuum at  $\sim 300$  K. The 3D growth mode is caused by kinetics rather than substrate strain, due to the fact of NaCl homoepitaxy, the low mobility and high supersaturation of solutes at room temperature. In our MD simulations in the mid-level supersaturation solution ( $\sigma=24\%$ ), the 3D islanding mode is also observed, though the size of islands are smaller. This result also helps us to understand why the growth of crystals from solution is so time-consuming and why there is step bunching on a growing crystal face.<sup>3</sup>

#### IV. CONCLUSIONS

In conclusion, the initial stage of the NaCl crystallization process at the water-NaCl (001) interface from a supersaturated NaCl solution has been investigated by molecular dynamics simulations. We find from our statistical calculations that the critical nucleus consists of two atoms: one Na<sup>+</sup> ion and one Cl<sup>-</sup> ion. Although this facilitates nucleation rates, the subsequent growth of these small nuclei is much affected by surrounding water molecules and thus slows down. The Na<sup>+</sup>

ions from the supersaturated solution show a higher deposition rate than the  $\text{Cl}^-$  ions due to the presence of a relatively stable water network on the NaCl (001) surface and the difference in the hydration force. This is different from the case of NaCl epitaxy in the vacuum, and reveals the importance of water molecules involved into crystal growth at the water-solid interfaces. We also found that both  $\text{Na}^+$  and  $\text{Cl}^-$  ions can serve as nucleation centers of stable nuclei, which is different from the case of homogeneous nucleation in NaCl supersaturated solution.<sup>10</sup> Based on the different deposition characteristics of  $\text{Na}^+$  and  $\text{Cl}^-$  ions, a new mechanism that contributes to nucleation and growth of NaCl crystals from solutions has been proposed—the unbalance of Coulomb interactions between the surface and solution, which may induce another driving force for the deposition of solute  $\text{Cl}^-$  ions. At high solution concentration and room temperature, the epitaxial solutes take a 3D island growth mode. Although the number of particles and simulation time are limited by the increase of computational demand, our results offer insight into the nucleation mechanism at the NaCl-water interface, and have implications towards the improvement of crystal growth from aqueous solutions.

## ACKNOWLEDGMENTS

The authors are indebted to Professor E. G. Wang and Professor Shiwu Gao for their insightful discussion and improvement of the text. They also thank Professor Zhenyu Zhang and Professor Feng Liu for their helpful discussion. This work was partly supported by NSF, MOST, and CAS of China for one of the authors (Y.Y.) and U.S. NSF for the other author (S.M.).

## APPENDIX: THE RELATIONSHIP BETWEEN CRITICAL SIZE AND SOLUTION SUPERSATURATION

We show the relationship between the size of critical nuclei and the level of solution supersaturation.

When a crystallite containing  $n$  particles is formed on the substrate, the change in Gibbs free energy is<sup>5,29</sup>

$$\Delta G(n) = n\Delta\mu + (\gamma_{\text{ws}} - \gamma_{\text{wl}})A_{\text{ws}} + \gamma_{\text{ls}}A_{\text{ls}}, \quad (\text{A1})$$

where  $\Delta\mu = \mu_{\text{s}} - \mu_{\text{l}}$  is the difference of chemical potential between solid and liquid/solution phases,  $\gamma$  is the liquid/solid free energy density, and  $A$  is the newly created surface areas at the interface. The subscripts  $w$ ,  $l$ , and  $s$  represent the substrate, the liquid (or solution), and the solid, respectively. From liquid (or solution) state to solid state,  $\Delta\mu < 0$ . In our case, the solid and the substrate are both NaCl, so  $\gamma_{\text{ws}} = 0$ ,  $\gamma_{\text{wl}} = \gamma_{\text{ls}} = \gamma$ , and  $\Delta G(n)$  is reduced to

$$\Delta G(n) = n\Delta\mu + \gamma(A_{\text{ls}} - A_{\text{ws}}). \quad (\text{A2})$$

Generally, the difference of interfacial area ( $A_{\text{ls}} - A_{\text{ws}}$ ) can be written as the function of particle number  $n$ ,

$$(A_{\text{ls}} - A_{\text{ws}}) = A(n) = \lambda n^{2/3}, \quad (\text{A3})$$

where  $\lambda$  is the shape factor of the crystallite at the interface.

For a rectangular prism crystallite with the length  $L$ , width  $c_1L$ , and thickness  $c_2L$  ( $c_1$  and  $c_2$  are real numbers), its volume  $V = c_1c_2L^3 = n\Omega$ , and

$$L = \left( \frac{n\Omega}{c_1c_2} \right)^{1/3}, \quad (\text{A4})$$

$$\begin{aligned} (A_{\text{ls}} - A_{\text{ws}}) &= A(n) = 2(1 + c_1)c_2L^2 \\ &= 2(1 + c_1)c_2 \left( \frac{n\Omega}{c_1c_2} \right)^{2/3} = \lambda n^{2/3}, \end{aligned} \quad (\text{A5})$$

thus

$$\lambda = 2(1 + c_1)c_2 \left( \frac{\Omega}{c_1c_2} \right)^{2/3}, \quad (\text{A6})$$

where  $\Omega = a^3/4$  is the volume of one NaCl ion pair occupies in the solid phase, and  $a = 5.67 \text{ \AA}$  is the lattice constant of NaCl crystal.

Similarly, for a triangle prism crystallite with the same edge lengths and thickness, the shape factor is  $\lambda = [(1 + c_1) + \sqrt{1 + c_1^2}]c_2(2\Omega/c_1c_2)^{2/3}$ .

At the critical size, one has  $\partial\Delta G/\partial n = 0$ , which gives

$$n_c = - \left( \frac{2\lambda\gamma}{3\Delta\mu} \right)^3. \quad (\text{A7})$$

The relationship between  $\Delta\mu$  and supersaturation  $\sigma$  is:<sup>17</sup>

$$\Delta\mu = -k_B T \ln(1 + \sigma). \quad (\text{A8})$$

So

$$n_c = \left[ \frac{2\lambda\gamma}{3k_B T \ln(1 + \sigma)} \right]^3. \quad (\text{A9})$$

The critical size  $n_c$  will increase when the supersaturation  $\sigma$  is decreased.

<sup>1</sup>J. Anwar and P. K. Boateng, *J. Am. Chem. Soc.* **120**, 9600 (1998).

<sup>2</sup>Y. Georgalis, A. M. Kierzek, and W. Saenger, *J. Phys. Chem. B* **104**, 3405 (2000).

<sup>3</sup>M. Asta, F. Spaepen, and J. F. van der Veen, *MRS Bull.* **29**, 920 (2004).

<sup>4</sup>T. Koishi, K. Yasuoka, and T. Ebisuzaki, *J. Chem. Phys.* **119**, 11298 (2003).

<sup>5</sup>S. Auer and D. Frenkel, *Phys. Rev. Lett.* **91**, 015703 (2003).

<sup>6</sup>S. Auer and D. Frenkel, *Nature (London)* **409**, 1020 (2001).

<sup>7</sup>S. Auer and D. Frenkel, *Nature (London)* **413**, 711 (2001).

<sup>8</sup>A. Cacciuto, S. Auer, and D. Frenkel, *Nature (London)* **428**, 404 (2004).

<sup>9</sup>H. Ohtaki and N. Fukushima, *Pure Appl. Chem.* **63**, 1743 (1991).

<sup>10</sup>D. Zahn, *Phys. Rev. Lett.* **92**, 040801 (2004).

<sup>11</sup>J. A. Venables, *Philos. Mag.* **27**, 697 (1973).

<sup>12</sup>J. Maddox, *Nature (London)* **378**, 231 (1995).

<sup>13</sup>E. Oyen and R. Hentschke, *Langmuir* **18**, 547 (2002).

<sup>14</sup>D. A. Case, D. A. Pearlman, J. W. Caldwell *et al.*, AMBER 6, University of California, San Francisco, 1999.

<sup>15</sup>Y. Yang, S. Meng, L. F. Xu, E. G. Wang, and S. W. Gao, *Phys. Rev. E* **72**, 012602 (2005).

<sup>16</sup>*CRC Handbook of Chemistry and Physics*, 77th ed., edited by D. R. Lide (CRC Boca Raton, Florida, 1996).

<sup>17</sup>J. Garside, A. Mersmann, and J. Nyvlt, *Measurement of Crystal Growth and Nucleation Rates*, 2nd ed. (IChemE, UK, 2002).

<sup>18</sup>W. L. Jorgensen, J. Chandrasekhar, J. D. Madura, R. W. Impey, and M. L. Klein, *J. Chem. Phys.* **79**, 926 (1983).

<sup>19</sup>M. Patra and M. Karttunen, *J. Comput. Chem.* **25**, 678 (2004). (The size and energy parameters of  $\text{Na}^+$  and  $\text{Cl}^-$  are the same in PARM94 and PARM99 force fields).

<sup>20</sup>D. E. Smith and L. X. Dang, *J. Chem. Phys.* **100**, 3757 (1994).

- <sup>21</sup>T. Darden, D. York, and L. Pedersen, *J. Chem. Phys.* **98**, 10089 (1993).
- <sup>22</sup>U. Essmann, L. Perera, M. L. Berkowitz, T. Darden, H. Lee, and L. G. Pedersen, *J. Chem. Phys.* **103**, 8577 (1995).
- <sup>23</sup>J. P. Ryckaert, G. Ciccotti, and H. J. C. Berendsen, *J. Comput. Phys.* **23**, 327 (1977).
- <sup>24</sup>H. J. C. Berendsen, J. P. M. Postma, W. F. van Gunsteren, A. DiNola, and J. R. Haak, *J. Chem. Phys.* **81**, 3684 (1984).
- <sup>25</sup>K. F. Kelton, *Solid State Physics*, edited by H. Ehrenreich and D. Turnbull (Academic, New York, 1991), Vol. 45, pp. 75–178.
- <sup>26</sup>R. G. S. Pala and F. Liu, *Phys. Rev. Lett.* **95**, 136106 (2005).
- <sup>27</sup>D. van der Spoel, P. J. van Maaren, and H. J. C. Berendsen, *J. Chem. Phys.* **108**, 10220 (1998); P. Mark and L. Nilsson, *J. Phys. Chem. A* **105**, 9954 (2001).
- <sup>28</sup>J. Arsic, D. M. Kaminski, N. Radenovic, P. Poodt, W. S. Graswinckel, H. M. Cuppen, and E. Vlieg, *J. Chem. Phys.* **120**, 9720 (2004).
- <sup>29</sup>D. Turnbull, *J. Chem. Phys.* **18**, 198 (1950).